

Congenital thoracic arterial anomalies in adults: a CT overview

Afra Yıldırım, Nevzat Karabulut, Serap Doğan, Duygu Hersek

ABSTRACT

Congenital thoracic arterial anomalies can be incidentally detected in adults from imaging studies performed for other indications. Multidetector computed tomography plays a critical role in the noninvasive assessment of these anomalies and associated cardiac, mediastinal, or parenchymal changes by providing volumetric data. Radiologists should be familiar with imaging findings of these anomalies to avoid misinterpretation and to establish accurate diagnosis. In this article, we review the imaging characteristics of congenital aortic, pulmonary, and aortopulmonary anomalies with an emphasis on multidetector computed tomography findings. We illustrate the CT findings of congenital arterial anomalies such as double aortic arch, right aortic arch, aortic coarctation, pseudo-coarctation, interrupted aortic arch, interruption (absence) of the pulmonary artery, pulmonary artery sling, pulmonary artery stenosis, transposition of great vessels, truncus arteriosus, aortopulmonary window, and patent ductus arteriosus.

Key words: • arteries • congenital abnormalities • adult • tomography, X-ray computed

Thoracic arterial anomalies can be isolated or associated with congenital heart diseases. Many of these findings are clinically silent unless they are associated with esophageal or airway obstruction or cardiac anomalies. Thoracic arterial anomalies can be classified as the following: systemic and pulmonary arterial anomalies, aortopulmonary anomalies, or pulmonary arteriovenous malformations. Cross-sectional imaging techniques, such as echocardiography, magnetic resonance imaging (MRI), and multidetector computed tomography (MDCT), have enabled noninvasive diagnosis of vascular anomalies. The use of MDCT is advantageous because it makes a wider anatomic field visible and its higher resolution allows quicker and more reliable detection of arterial anomalies. In addition, maximum intensity projection images obtained by MDCT angiography display vascular anomalies, whereas minimum intensity projection virtual bronchoscopy images portray accompanying airway anomalies. However, there are disadvantages to the use of MDCT, the most important of which is radiation exposure (1–4).

Technique

We use 16-section MDCT scanners (Brilliance 16, Philips Medical Systems, Cleveland, Ohio, USA; and LightSpeed 16, GE Healthcare, Milwaukee, Wisconsin, USA). The parameters for thoracic computed tomography (CT) angiography are the following: beam collimation, 16×0.75 mm; pitch, 1.75; slice thickness, 1.25 mm; and reconstruction interval, 0.75 mm. Images are obtained in the supine position. In adult patients, the tube current is set to 220 mA, and the tube voltage is 120 kV. Scans are obtained during a single breath-hold. Approximately 100–110 mL of nonionic low-osmolarity contrast material with a concentration of 350 mg I/mL is injected with an automatic injector into an antecubital vein at a flow rate of 4 mL/s. The scan delay is set using automated bolus-tracking software, and the acquisition is triggered automatically when the contrast material reached the region of interest. The images are sent to a workstation (MxViewexp, release 4.01, Philips Medical Systems; or Advantage ADW 4.2, GE Healthcare). Conventional transverse images, multiplanar reformatted reconstructions, maximum intensity projections and volume-rendered three-dimensional (3D) images are generated for evaluation.

Systemic arterial anomalies

Aortic arch anomalies constitute the most common type of congenital anomalies of the thoracic aorta, whereas anomalies of the descending aorta are very rare (1, 2, 5, 6).

Left aortic arch with aberrant right subclavian artery

Aberrant right subclavian artery is the most commonly encountered aortic arch anomaly, which is seen in 5% of the population. This anomaly

From the Department of Radiology (A.Y. ✉ afra_yildirim@hotmail.com, S.D.), Erciyes University School of Medicine, Kayseri, Turkey; the Department of Radiology (N.K., D.H.), Pamukkale University School of Medicine, Denizli, Turkey.

Received 25 May 2011; revision requested 21 June 2011; revision received 2 August 2011; accepted 4 August 2011.

Published online 6 October 2011
DOI 10.4261/1305-3825.DIR.4645-11.1

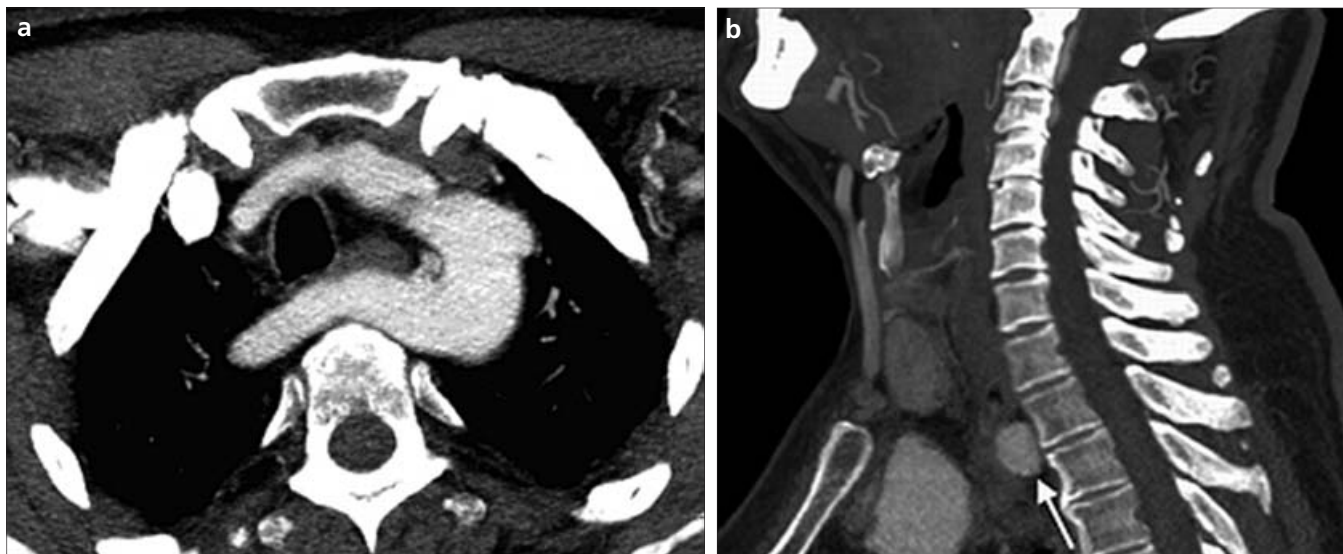


Figure 1. a, b. Aneurysm of the aberrant right subclavian artery in an adult male presenting with dysphagia. Contrast-enhanced transverse CT image (a) shows an aberrant right subclavian artery that arises as the last branch of a left-sided aortic arch. Sagittal reformatted CT image (b) demonstrates compression of the esophagus by the aberrant right subclavian artery (arrow).

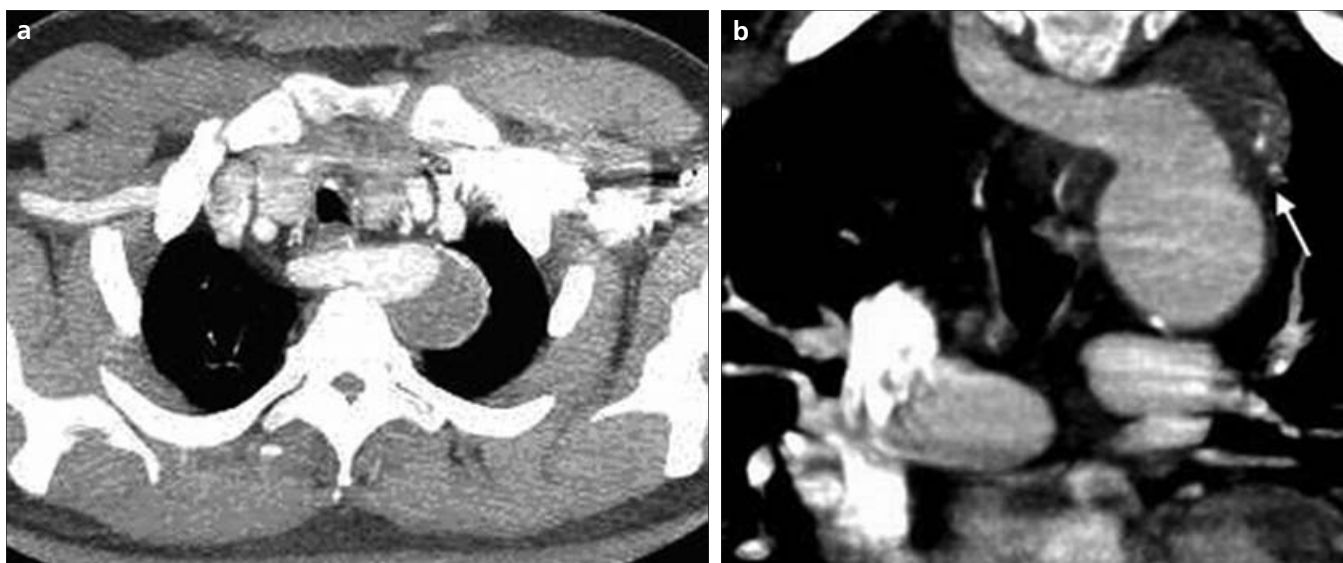


Figure 2. a, b. Aberrant right subclavian artery in a 64-year-old male. Contrast-enhanced transverse (a) and coronal reformatted (b) CT images demonstrate a right aberrant subclavian artery with partially thrombosed aneurysm (arrow, b) arising from a Kommerell's diverticulum.

is caused by interruption of the right aortic arch between the right common carotid and the right subclavian artery. The condition is generally asymptomatic; however, rarely it may cause dysphagia (dysphagia lusoria). Aberrant right subclavian artery arises as the last branch of the aorta; in 80% of patients, it runs behind the esophagus, but it may also pass in front of the esophagus (15%) or trachea (5%). The residue of the right dorsal aortic artery root may be seen as a focal enlargement (known as Kommerell's diverticulum) at its origin. This diverticulum can develop into an aneurysm. This anomaly can

simulate retrotracheal space-occupied lesions, such as lymphadenopathy, esophageal abnormalities, mediastinal tumors, and infections on chest radiography and unenhanced CT. Contrast enhanced MDCT clearly demonstrates the aberrant artery, diverticulum, and aneurysm (Figs. 1, 2) (2, 7–9).

Double aortic arch

Double aortic arch is the most common cause of vascular ring and occurs due to the persistence of both left and right fourth aortic arches. The right and left arches arise from the ascending aorta; they then encircle the

esophagus and trachea to join and then take off the common carotid and subclavian arteries. There are three forms of double aortic arch: right arch dominant (75%), left arch dominant (20%), and arches of the same size (5%). A portion of the arch is atretic in about one-third of cases (5, 10). The descending aorta is usually on the left side, but it may also be at the midline or on the right side. Left aortic arch may cause a complete vascular ring as a fibrous, atretic segment, and surgery is mandatory in the early stages due to symptoms of esophageal and tracheal compression (2).

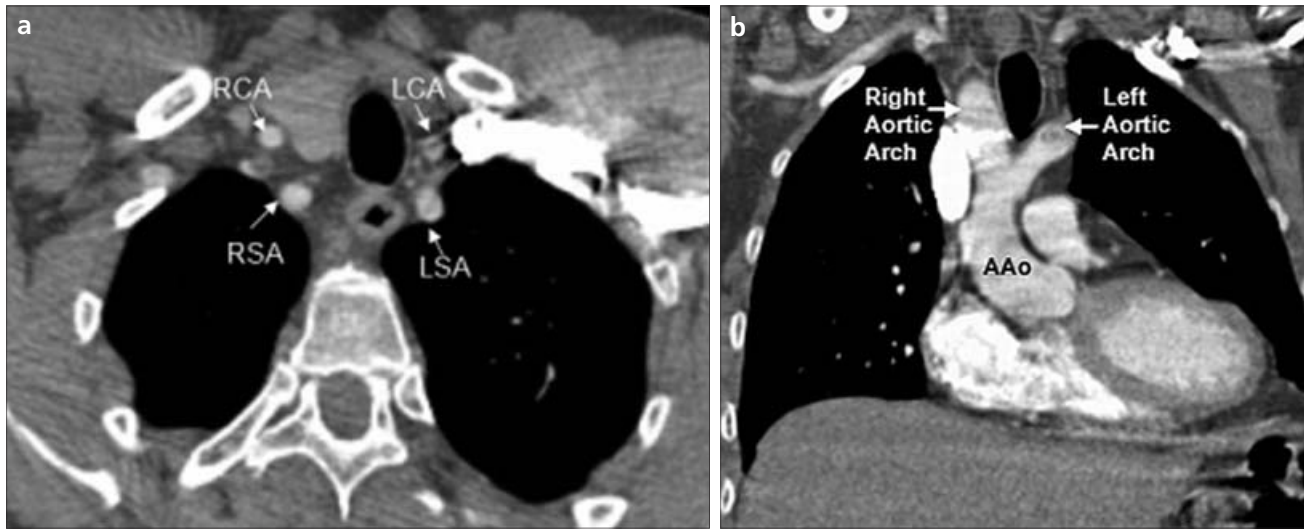
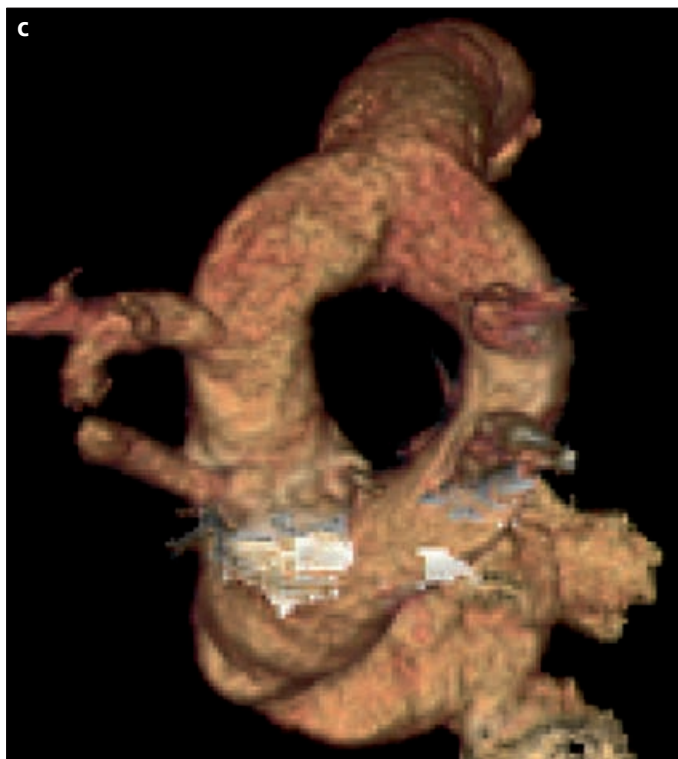


Figure 3. a–c. Double aortic arch in a 31-year-old male. Contrast-enhanced transverse (a) CT image shows symmetrical arch vessels in the thoracic inlet. Coronal reformatted (b) and volume rendering (c) CT images reveal a double aortic arch. RSA, right subclavian artery; RCA, right common carotid artery; LSA, left subclavian artery; LCA, left common carotid artery; AAo, ascending aorta.



Contrast-enhanced MDCT shows esophageal and tracheal stenosis, and four branches (two carotid arteries and two subclavian arteries) (Fig. 3). Coronal and 3D images are useful to display double aortic arch. When both arches have similar diameters, phase-contrast velocity mapping on MRI may help in planning for surgery (7).

Right aortic arch

Right aortic arch occurs due to the persistence of the fourth right aortic arch. Symptoms may occur due to tracheal and, in some cases, esophageal compression. Types of right aortic arch vary according to the interruption level of the left aortic arch. In type 1, a right aortic arch occurs with an aberrant left subclavian artery, whereas a subclavian artery with mirror-image branching or an isolated left subclavian artery (which arises from the left pulmonary artery via the ductus arteriosus) accompanies a right aortic arch in types 2 and 3, respectively (Fig. 4). Type 1 is the most common right aortic arch anomaly, and it is the second most common cause of a vascular ring. The ring is completed by the left-sided arterial ligament (11). The concomitance of type 1 with congenital heart disease is rare. However, congenital heart disease, such as tetralogy of Fallot, truncus arteriosus, and ventricular septal defect (VSD), accompanies type 2 anomaly in 98% of cases. Because the arterial ligament is on the

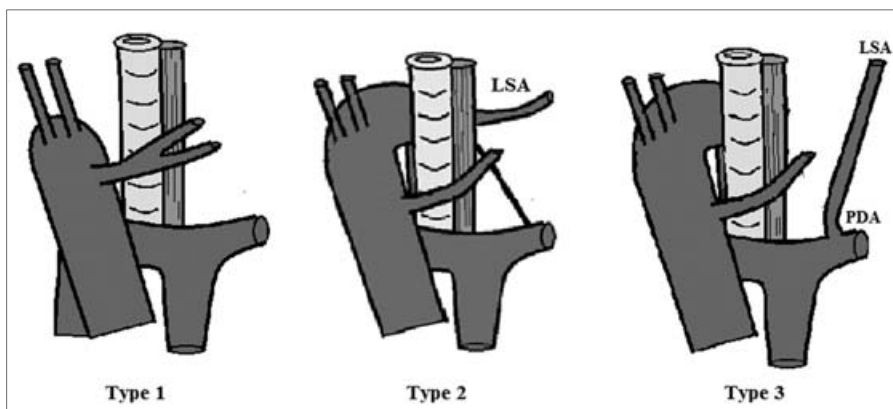


Figure 4. Types of right aortic arch. LSA, left subclavian artery; PDA, patent ductus arteriosus. Please refer to the text for a detailed explanation.

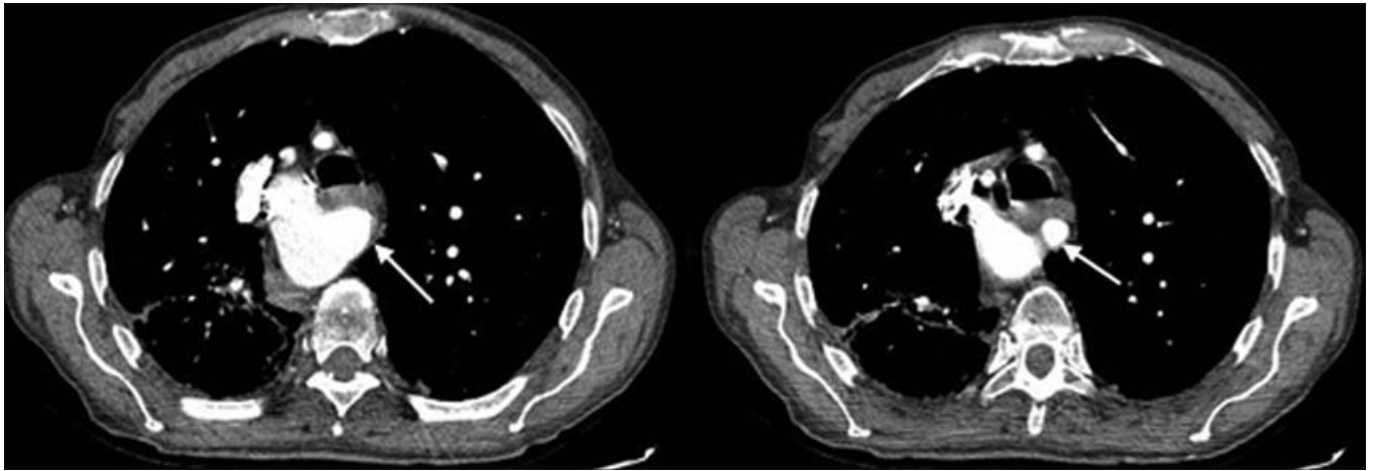


Figure 5. Right aortic arch in a 73-year-old male. Consecutive contrast-enhanced axial CT images display the right aortic arch and the aberrant left subclavian artery (arrow).

left side, no vascular ring is present in a right aortic arch with mirror-image branching.

Left subclavian artery is the last branch in the type 1 anomaly. This can cause dysphagia by compressing the esophagus. There may be a Kommerell's diverticulum at the origin of the left subclavian artery (11, 12).

This anomaly can mimic a mediastinal mass on chest radiography and non-contrast CT and is observed as a round-shaped mass at the right lateral side of the trachea. In addition, right tracheal deviation may be seen. CT or MRI is necessary when there are symptoms of a vascular ring. MDCT can clearly demonstrate right aortic arch, aberrant subclavian artery, diverticulum and tracheal/esophageal stenosis (Fig. 5) (12).

Aortic coarctation

Aortic coarctation is a congenital narrowing at the junction of the aortic arch and the descending aorta and accounts for 5%–10% of all congenital heart diseases. A bicuspid aortic valve is seen in 85% of cases. It may occur sporadically or be associated with chromosomal abnormalities. In Turner syndrome, there is a 20%–36% increased risk of coarctation. Coarctation may cause congestive heart failure, hypertension and blood pressure gradients between lower and upper extremities. Intimal thickening and disruption of elastic tissue occur at the distal part, which cause a predisposition to infective endarteritis, intimal dissection, and aneurysm (2, 5, 13)

There are two types of aortic coarctation: preductal (infantile) and postductal (adult). In the preductal type,

segmental narrowing of the aortic arch due to tubular hypoplasia beginning at the level of origin of the brachiocephalic artery accompanies focal narrowing distal to the ductus arteriosus. In the postductal type, there is a focal narrowing at the distal part of the ductus arteriosus or left subclavian artery (2, 5, 13).

In aortic coarctation, systemic collateral vessels develop to supply the low-pressure areas distal to the narrowing. Internal mammary (thoracic), vertebral, thoracoacromial, and descending scapular arteries are connected with the descending aorta via the intercostal arteries. Additionally, anastomoses between an internal mammary artery and external iliac arteries via superior and inferior epigastric arteries develop (2).

MDCT demonstrates the location and length of the coarctation, the presence of post-stenotic dilatation, collaterals and hypoplasia of the arch (Fig. 6). Moreover, MDCT can readily detect complications, such as dissection, aneurysm, and rupture (14, 15).

Aortic pseudocoarctation

Aortic pseudocoarctation is the presence of kinking in the aortic arch at the level of the arterial ligament. This anomaly is secondary to fusion failure of the third to sixth dorsal aortic segments. There is narrowing and turbulence at the level of the kinking. As in coarctation, there is a predisposition to aneurysm and dissection (12). Pseudocoarctation is distinguished from coarctation by the lack of blood pressure gradient. CT and MRI delineate

elongation and higher localization of the descending aorta and aortic arch with kinking of the aorta distal to the origin of the left subclavian artery. The absence of significant stenosis and collateral vessels enables differentiation from true coarctation (Fig. 7). Phase-contrast MRI can demonstrate the absence of a pressure gradient (2).

Interrupted aortic arch

Interrupted aortic arch is complete discontinuity of the lumen. This abnormality is responsible for less than 1.5% of all congenital cardiac malformations and can be classified into three types according to the localization of the interruption. There is an interruption distal to the left subclavian artery in type A (13%), between the left subclavian and common carotid artery in type B (84%) and between the left common carotid and brachiocephalic artery in type C (4%) (Fig. 8) (16). Patent ductus arteriosus (PDA) invariably co-exists; thus, the PDA provides distal aortic flow. VSD may be concurrently present. A right-sided descending aorta with an interrupted aortic arch is always present in Di George syndrome. MDCT angiography shows the location of the interruption and collateral vessels (Fig. 9). MRI with steady state free precession sequences and magnetic resonance (MR) angiography are useful in the assessment of thoracic aorta, great vessels, concomitant cardiac anomalies, and valve function (7, 16).

Cervical aortic arch

Cervical aortic arch is caused by the persistence of the third aortic arch

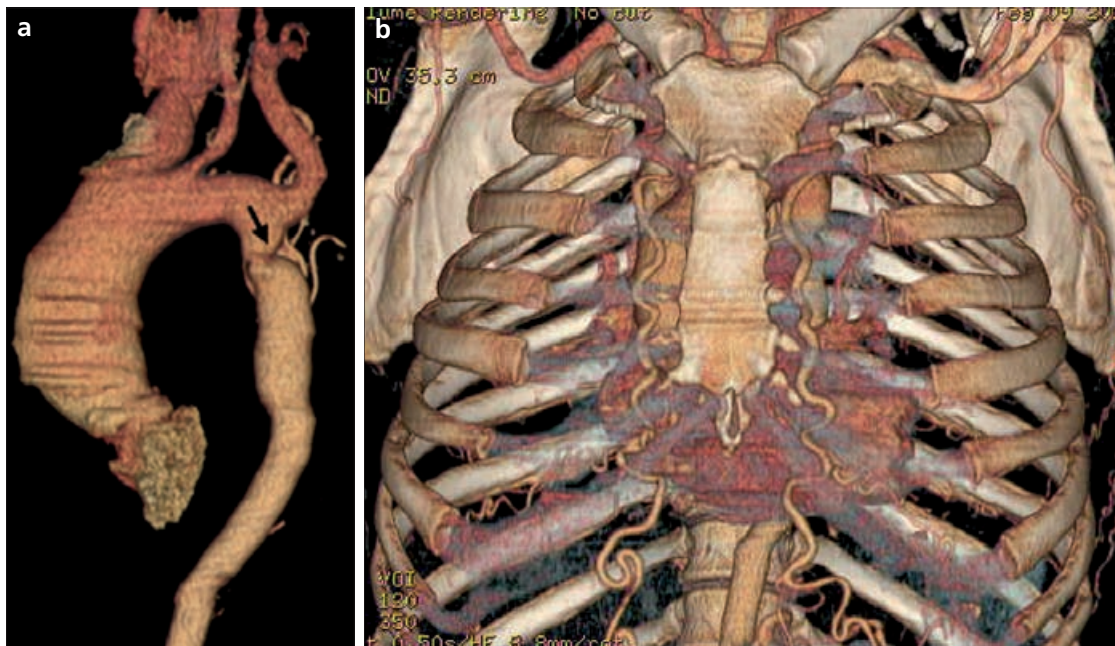


Figure 6. a, b. Aortic coarctation in a 49-year-old male. Lateral (a) and anterior (b) volume rendering CT images of the postductal aortic coarctation (arrow, a). The enlarged internal mammary arteries and dilated posterior collateral intercostal arteries can be observed.

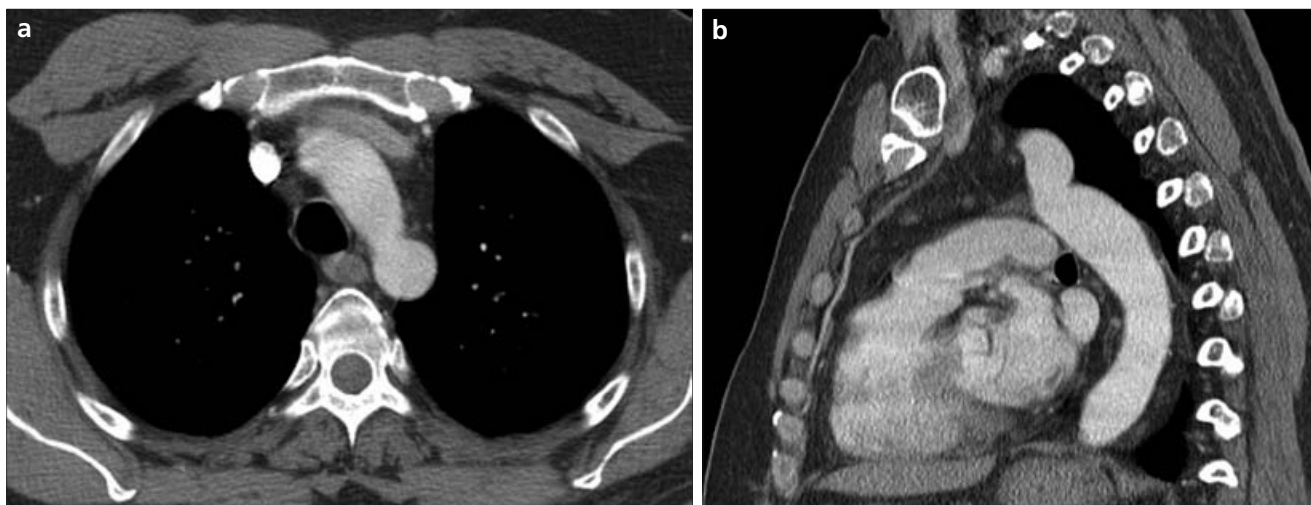


Figure 7. a, b. Pseudocoarctation of the aorta in a 63-year-old woman with Turner syndrome. Contrast-enhanced transverse (a) and sagittal reformatted (b) CT images show elongated descending aorta with kinking of the elongated descending aorta distal to the origin of the left subclavian artery. (Courtesy of Lawrence R. Goodman, MD, Medical College of Wisconsin, Milwaukee, Wisconsin, USA.)

instead of the fourth. Cervical aortic arch is an elongated aortic arch that extends into the soft tissues of the neck before turning downward on itself to become the descending aorta (17). This anomaly is usually asymptomatic; however, dysphagia and respiratory symptoms may be present. This anomaly may also be a part of various syndromes, such as Di George or Turner syndromes (18). Clinically, a pulsatile supraclavicular mass is a characteristic finding (9). MDCT enables an accurate diagnosis by demonstrating the cervical extension of the arch.

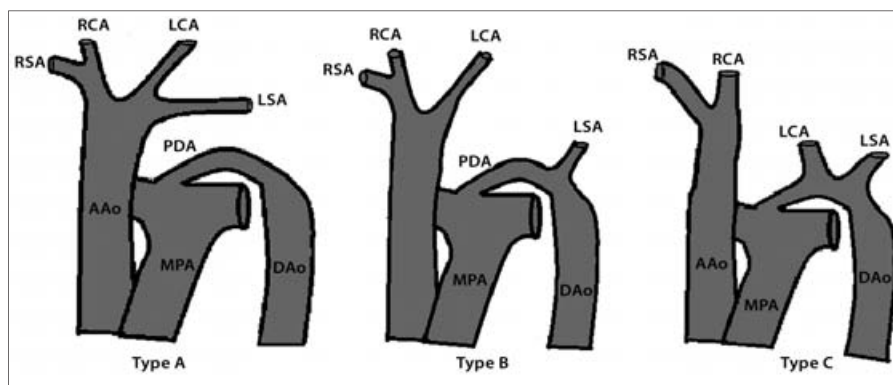


Figure 8. Types of aortic arch interruption. AAO, ascending aorta; DAO, descending aorta; MPA, main pulmonary artery; RSA, right subclavian artery; RCA, right common carotid artery; LSA, left subclavian artery; LCA, left common carotid artery; PDA, patent ductus arteriosus. Please refer to the text for a detailed explanation.

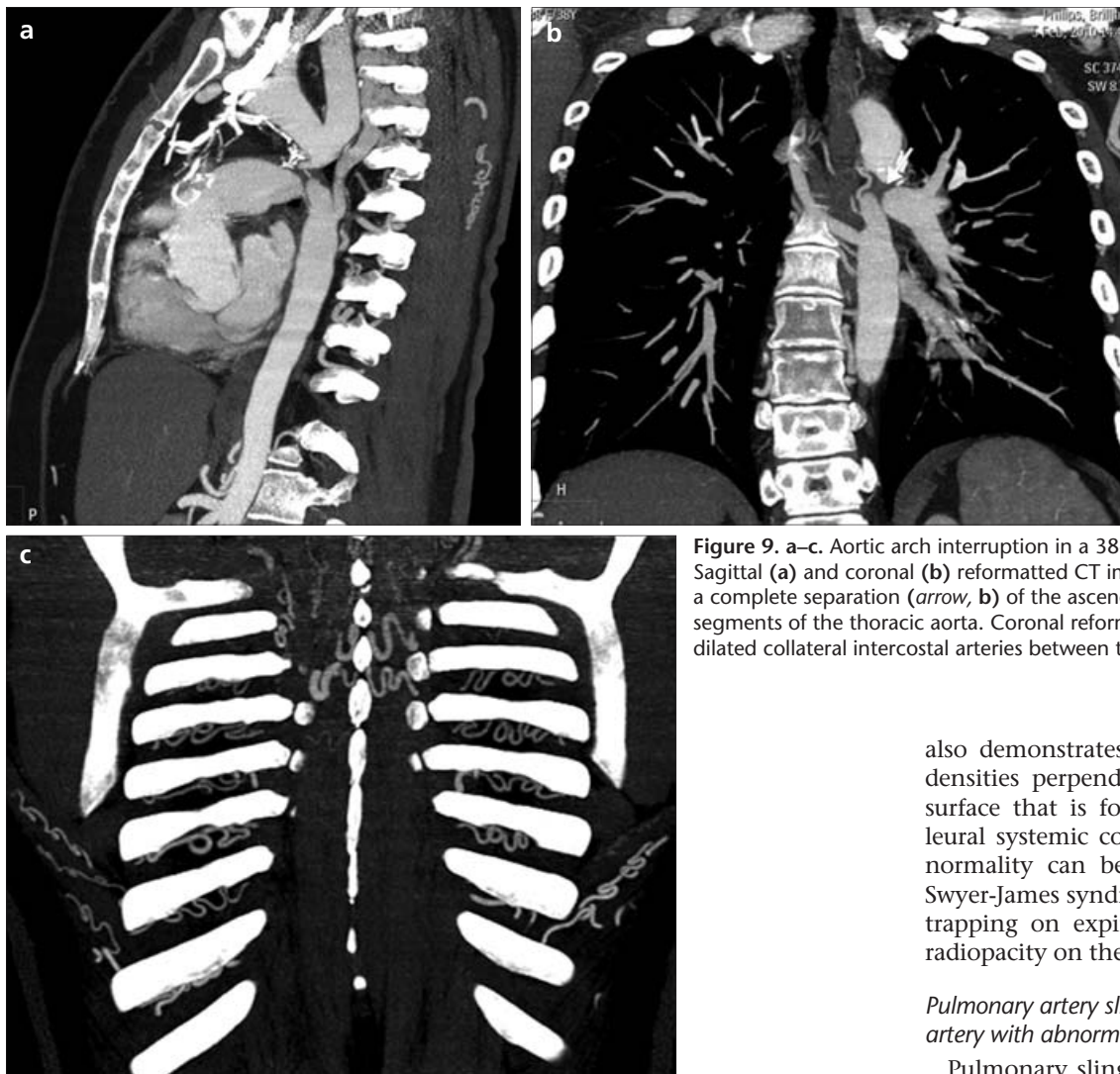


Figure 9. a–c. Aortic arch interruption in a 38-year-old female. Sagittal (a) and coronal (b) reformatted CT images clearly delineate a complete separation (arrow, b) of the ascending and descending segments of the thoracic aorta. Coronal reformatted (c) CT shows dilated collateral intercostal arteries between the third and eighth ribs.

Pulmonary arterial anomalies

Idiopathic dilatation of the pulmonary truncus

Idiopathic dilatation of the pulmonary artery is rare and asymptomatic. Generally, this abnormality is incidentally detected on chest radiography. To establish the diagnosis of idiopathic dilatation, right ventricle and pulmonary artery pressures should be normal, and cardiac and pulmonary diseases that can cause pulmonary hypertension should be excluded. This anomaly may involve the right or left pulmonary artery. A definitive diagnosis can be established with MDCT, MRI, and echocardiography (19).

Interruption (absence) of the pulmonary artery

Interruption of the pulmonary artery is a rare anomaly, and the term

“interruption” is used instead of “absence” because a part of the pulmonary artery is usually present within the lung parenchyma (19). In a proximal interruption, the pulmonary artery ends blindly at the hilum, and pulmonary blood supply is delivered by bronchial or transpleural systemic arteries. Involvement of the right side is mainly isolated and is more common than the left. Left-sided involvement is usually accompanied by right aortic arch and congenital heart diseases. Recurrent pulmonary infections, mild exercise dyspnea, and hemoptysis are the most common symptoms (2, 3). Pulmonary hypertension, which is present in 19%–25% of patients, is the most important prognostic predictor. Contrast-enhanced CT facilitates diagnosis by demonstrating the absence of the pulmonary artery around the small hilum or proximal interruption (Fig. 10). CT

also demonstrates linear parenchymal densities perpendicular to the pleural surface that is formed by the transpleural systemic collaterals (3). This abnormality can be differentiated from Swyer-James syndrome by its lack of air trapping on expiration and increased radiopacity on the affected side (20).

Pulmonary artery sling (left pulmonary artery with abnormal origin)

Pulmonary sling describes a left pulmonary artery that arises from the posterior aspect of the right pulmonary artery and runs between the esophagus and the trachea to the left hilum. The arterial ligament completes the vascular ring, including the trachea. There are two types of pulmonary slings. In type 1, the carina is in its normal location at the level of the T4–T5 intervertebral disc. In this type, the proximal part of the left pulmonary artery compresses the trachea or the right main bronchus. This type exhibits indentation on the anterior wall of the esophagus, and functional narrowing is rare. In type 2, a reverse T-shaped carina is located at a lower level (at the level of T6), and there is bridging between the horizontally oriented main bronchi (2, 3, 19). In type 2, there is an O-shaped complete cartilage instead of a U-shaped post-membranous component. Therefore, a long segment of tracheal stenosis (ring-sling complex) is seen (4). Anomalies, such as tracheomalacia, tracheal

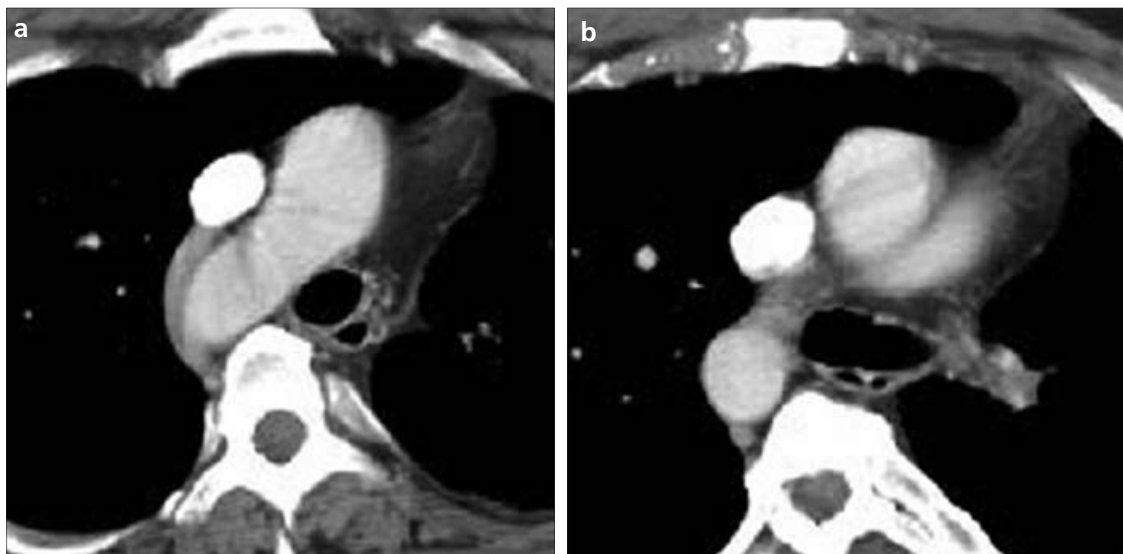


Figure 10. a, b. Interrupted left pulmonary artery in a 20-year-old female. Contrast-enhanced transverse CT images show an absence of the left pulmonary artery associated with the right aortic arch. Note the collateral vessels in the left hilum.

bronchus, and abnormal pulmonary lobulation, may co-exist. Fifty percent of these patients have an accompanying congenital heart disease. Symptoms related to respiratory distress may occur in the early period (2). Diagnosis can be made by CT and MR angiography (Fig. 11). MDCT and virtual bronchoscopy can be used in the assessment of the trachea. On barium esophagography, a mass just above the carina between the trachea and esophagus can be seen (21).

Pulmonary artery stenosis

Pulmonary artery stenosis in adults is rare. Although it can be isolated, pulmonary artery stenosis is frequently associated with other congenital cardiac malformations. This abnormality is also associated with Williams syndrome, Ehlers-Danlos syndrome, Down syndrome, and *in utero* exposure to rubella. This anomaly may be solitary or multiple and can occur anywhere from the pulmonary valves to the peripheral branches (22, 23). MDCT clearly demonstrates the location and extent of pulmonary stenosis, poststenotic dilatation, or aneurysm, and displays accompanying cardiac and parenchymal changes (Fig. 12).

Aortopulmonary anomalies

Transposition of great vessels

This anomaly is the most common cyanotic congenital heart disease in newborns. Transposition of great vessels accounts for approximately 5%–7% of all congenital cardiac malformations



Figure 11. a, b. Pulmonary artery sling in a 42-year-old male. Unenhanced transverse CT images at the level of the distal trachea show the abnormal course of the left pulmonary artery (*arrowhead, b*) between the lower portion of the trachea and the esophagus (*asterisks, a and b*). (Courtesy of Recep Savaş, MD, Department of Radiology, Ege University School of Medicine, Izmir, Turkey.)

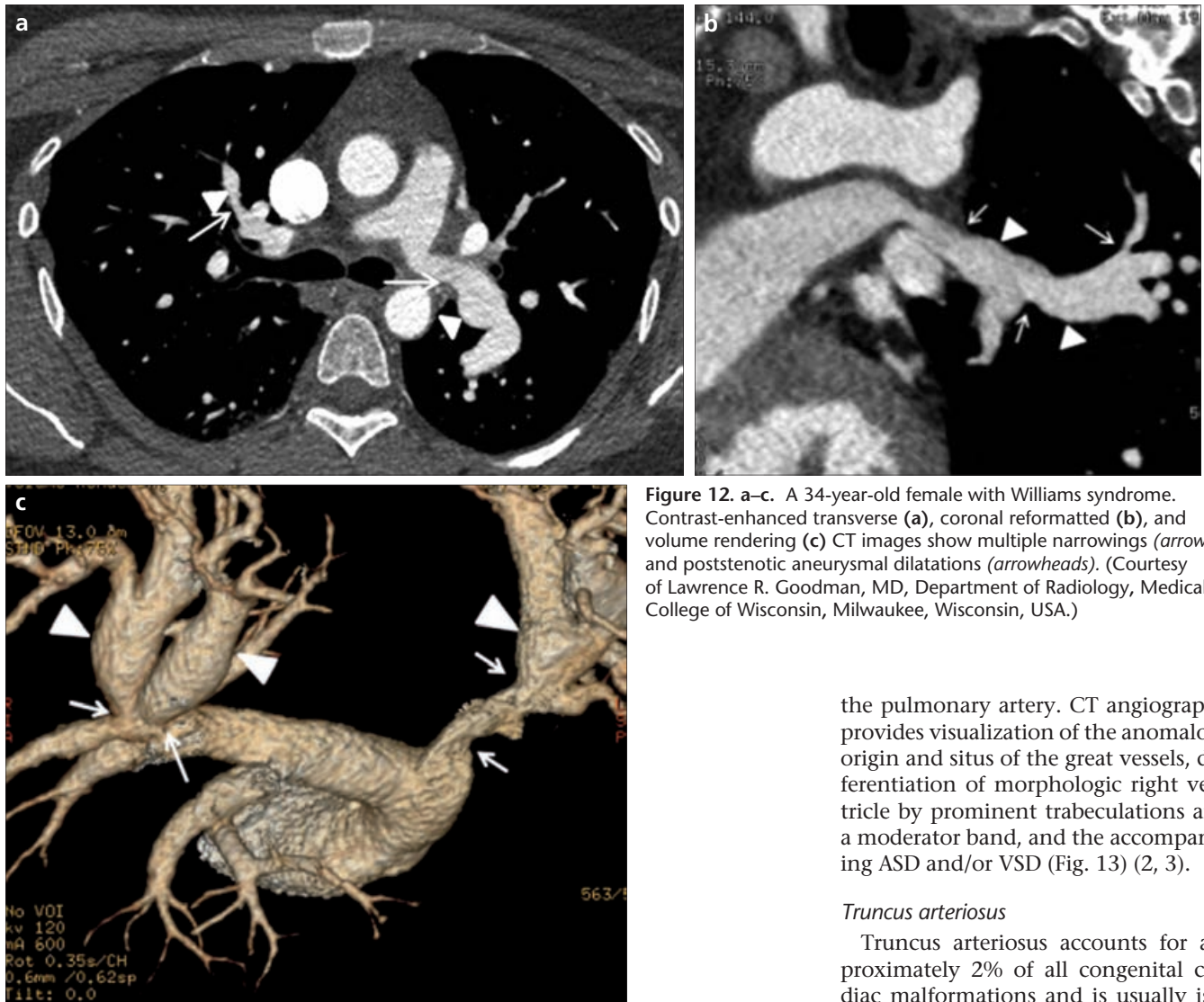


Figure 12. a–c. A 34-year-old female with Williams syndrome. Contrast-enhanced transverse (a), coronal reformatted (b), and volume rendering (c) CT images show multiple narrowings (arrows) and poststenotic aneurysmal dilations (arrowheads). (Courtesy of Lawrence R. Goodman, MD, Department of Radiology, Medical College of Wisconsin, Milwaukee, Wisconsin, USA.)

the pulmonary artery. CT angiography provides visualization of the anomalous origin and situs of the great vessels, differentiation of morphologic right ventricle by prominent trabeculations and a moderator band, and the accompanying ASD and/or VSD (Fig. 13) (2, 3).

Truncus arteriosus

Truncus arteriosus accounts for approximately 2% of all congenital cardiac malformations and is usually isolated. Truncus arteriosus occurs due to a failure in the separation of the trunk. The systemic, pulmonary, and coronary circulation originates from one vessel, and there is a single truncal valve, which is usually dysplastic and involves a variable number of leaflets, up to six. This condition can cause valvular regurgitation, stenosis or both. Absence of the right ventricular infundibular septum results in VSD. There are two classification systems for truncus arteriosus: Collett-Edwards and Van Praagh (5, 25). There are four types in each classification system based on the origins of the pulmonary arteries (Fig. 14). Collett-Edwards includes truncus arteriosus types 1–4: type 1, a single pulmonary artery trunk arises from the proximal left lateral aspect of the common trunk; type 2, the pulmonary trunk is absent and the separate right and left pulmonary arterial branches arise from the posterior or posterolateral aspect of the

and is due to impaired spiraling of the aorticopulmonary septum. The pulmonary artery originates from the morphologically left ventricle located on the right whereas the aorta arises from the morphologically right ventricle located on the left. In cases of transposition of great vessels, connections between the systemic and pulmonary circulation, such as atrial septal defect (ASD), VSD, or patent foramen ovale, are mandatory for life maintenance. A concurrent mirror-image right aortic arch is frequent. There are two forms of transposition of the great arteries: complete (dextro-transposition) and corrected (levo-transposition or double discordance). In complete transposition, the connections between the atria and ventricles are normal (atrioventricular concordance) but there is ventriculoarterial discordance, resulting in two independent

circulations. In dextro-transposition of the great arteries, the aorta is anterior and to the right of the pulmonary artery.

In corrected transposition of the great vessels, the connections between the atria and ventricles are discordant, with the right atrium connected to the left ventricle and the left atrium to the right ventricle (atrioventricular discordance). The great arteries are also transposed, with the aorta arising from the right ventricle and the pulmonary artery from the left (ventriculoarterial discordance). In this manner, “two anatomic wrongs (atrioventricular and ventriculoarterial discordances) make a physiologic right,” and deoxygenated systemic venous blood is routed to the lungs, and oxygenated pulmonary venous blood is routed to the body (2, 24). The aorta is located to the left side of

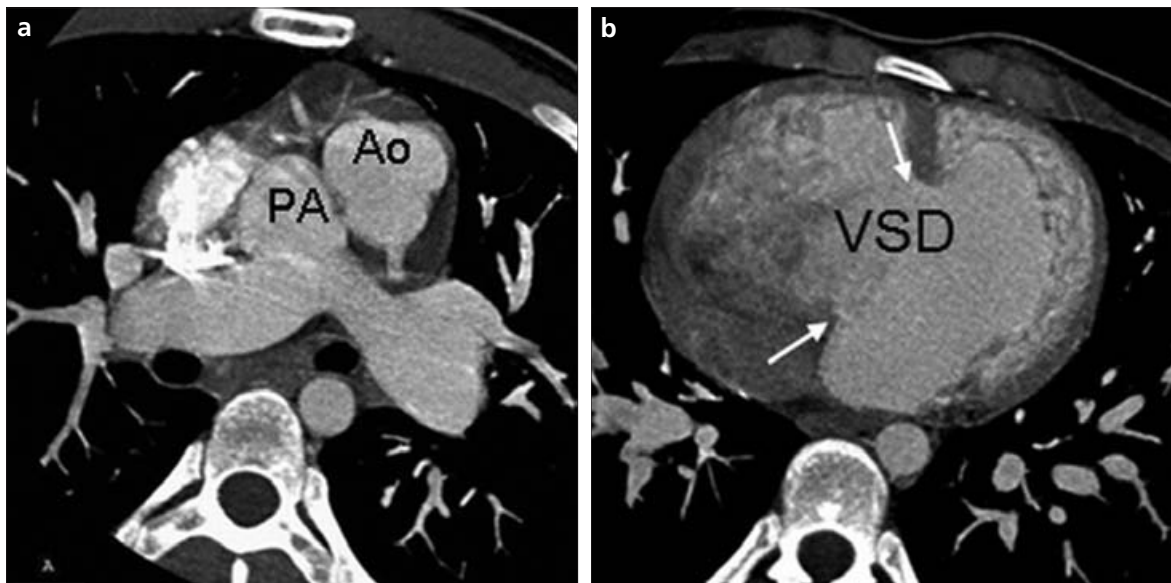


Figure 13. a, b. Corrected transposition of great vessels in an 18-year-old male. Contrast-enhanced transverse CT images demonstrate that the ascending aorta (Ao) is anterior to and at the left of the main pulmonary artery (PA) (a). Note the ventricle located on the left is morphologically the right ventricle with prominent trabeculations, and accompanying large ventricular septal defect (VSD) (arrows, b).

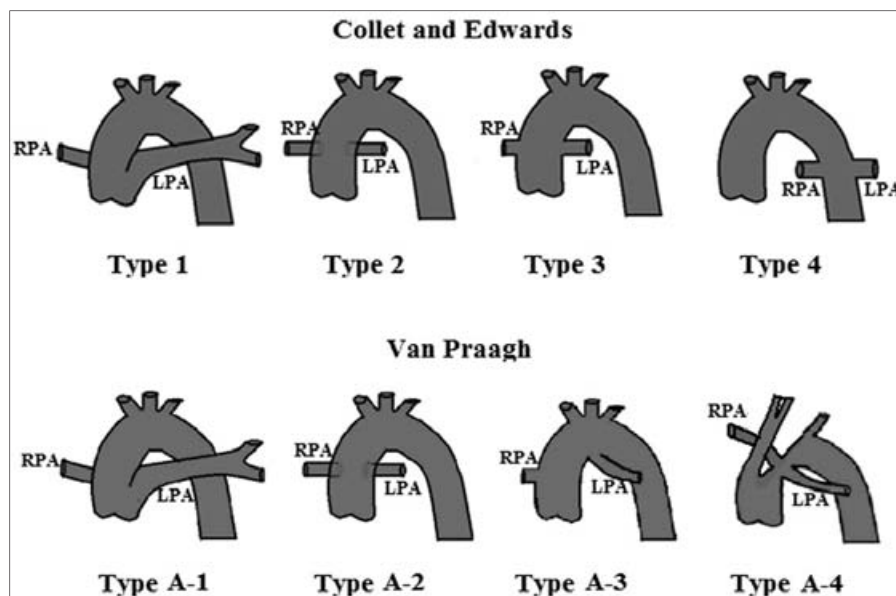


Figure 14. Classification systems of truncus arteriosus. RPA, right pulmonary artery; LPA, left pulmonary artery. Please refer to the text for a detailed explanation.

common trunk; type 3, the pulmonary trunk is absent and the right and left pulmonary branches arise from the lateral of the common trunk; and type 4, the pulmonary arteries arise from the descending aorta. In the Van Praagh system, types A1 and A2 truncus arteriosus are similar to Collett and Edwards types 1 and 2, respectively. In type A3, one branch of the pulmonary artery (usually the right) arises from the common trunk, with pulmonary blood supply to the other lung provided either by a pulmonary artery arising from the

aortic arch or by systemic to pulmonary arterial collaterals. In type A4, there is an associated interrupted aortic arch in addition to types 1 and 2. Contrast enhanced MDCT readily demonstrates suggested truncus arteriosus and accompanying ASD and VSD (Fig. 15).

Aortopulmonary window

The aortopulmonary window (APW) is a communication between the ascending aorta and the pulmonary trunk in the presence of two separate semilunar valves. The presence of both

aortic and pulmonary valves is important in distinguishing this anomaly from truncus arteriosus. APW is often complicated by associated cardiac defects. This anomaly accounts for approximately 1% of all congenital heart disease. Symptoms are related to the size of the window, the presence of associated defects and the evolution to pulmonary arterial hypertension. APW is mainly diagnosed by echocardiography and confirmed by cardiac angiography. MDCT angiography clearly demonstrates the location and size of the window (Fig. 16). CT also demonstrates signs of pulmonary arterial hypertension (5, 26).

Patent ductus arteriosus

PDA is a patency of the fetal duct between the distal main proximal left pulmonary artery and the descending aorta after birth. PDA is a normal pathway in fetal circulation that delivers deoxygenated blood from the right ventricle to the descending aorta. After birth, the PDA closes physiologically within 48 hours, and anatomical closure occurs within a few weeks after birth. This duct originates from the primitive sixth aortic arch. An extra-cardiac right-to-left shunt occurs due to insufficient closure of the duct (2). Echocardiography is used as the first line imaging modality in diagnosis. MRI and MDCT provide valuable information regarding localization and shape of the duct for pre-treatment assessment (Fig. 17).

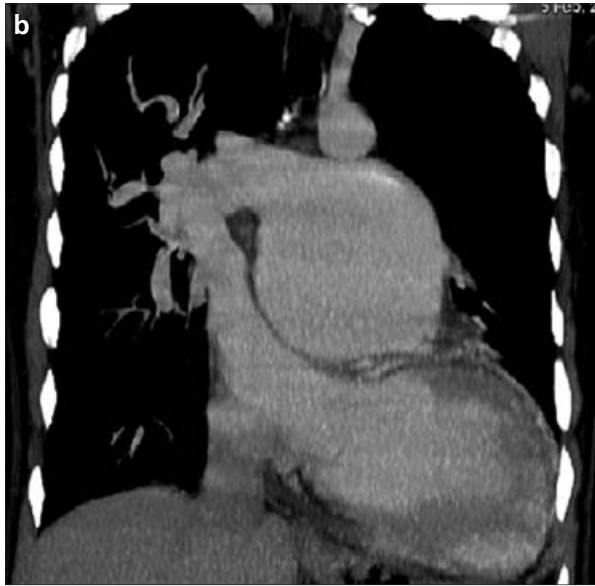
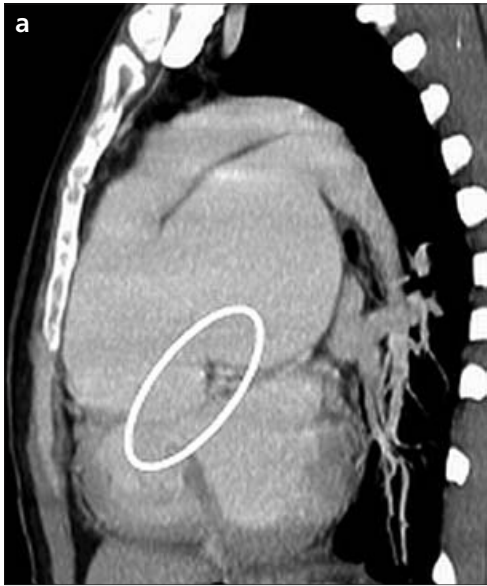


Figure 15. a, b. Truncus arteriosus in a 22-year-old female. Sagittal (a) and coronal (b) CT images show a single, large truncal vessel arising from the heart, which gives rise to the aorta and the pulmonary trunk (circle, a).



Figure 16. Aortopulmonary window in a 32-year-old male. Contrast-enhanced transverse CT at the level of the aortic valve shows communication between the aorta and pulmonary artery (arrows).



Figure 17. a, b. Patent ductus arteriosus in a 32-year-old male. Contrast-enhanced transverse (a) and sagittal (b) CT images show tubular structure (arrows, a and b) coursing between the aortic arch and the main pulmonary artery.

In conclusion, thoracic arterial anomalies may be detected incidentally on non-contrast CT scans performed for another reason and may simulate a mediastinal mass or lymphadenopathy. Familiarity with the radiologic findings of these anomalies is necessary to establish accurate diagnosis. When arterial anomaly is considered, further evaluation should be performed with contrast enhanced CT or MRI. By providing volumetric data, MDCT non-invasively reveals the anatomic course of these anomalies and concomitant cardiac, mediastinal, or parenchymal changes.

Conflict of interest disclosure

The authors declared no conflicts of interest.

References

1. Chung JH, Gunn ML, Godwin JD, Takasugi J, Kanne JP. Congenital thoracic cardiovascular anomalies presenting in adulthood: a pictorial review. *J Cardiovasc Comput Tomogr* 2009; 3:35–46.
2. Maldonado JA, Henry T, Gutiérrez FR. Congenital thoracic vascular anomalies. *Radiol Clin North Am* 2010; 48:85–115.
3. Lee EY, Boiselle PM, Cleveland RH. MDCT Evaluation of congenital lung anomalies. *Radiology* 2008; 247:632–648.
4. Zylak CJ, Eyler WR, Spizarny DL, Stone CH. Developmental lung anomalies in the adult: radiologic-pathologic correlation. *Radiographics* 2002; 22:25–43.
5. Kimura-Hayama ET, Meléndez G, Mendizábal AL, Meave-González A, Zambrana GF, Corona-Villalobos CP. Uncommon congenital and acquired aortic diseases: role of multidetector CT angiography. *Radiographics* 2010; 30:79–98.
6. Karadeli E, Ulu E. CT of double descending thoracic aorta in an adult female. *Diagn Interv Radiol* 2009; 15:179–181.
7. Weinberg PM. Aortic arch anomalies. *J Cardiovasc Magn Reson* 2006; 8:633–643.
8. Onbaş O, Kantarci M, Koplay M, et al. Congenital anomalies of the aorta and vena cava: 16-detector-row CT imaging findings. *Diagn Interv Radiol* 2008; 14:163–171.
9. Franquet T, Erasmus JJ, Giménez A, Rossi S, Prats R. The retrotracheal space: normal anatomic and pathologic appearances. *Radiographics* 2002; 22:231–246.
10. Lowe GM, Donaldson JS, Backer CL. Vascular rings: 10-year review of imaging. *Radiographics* 1991; 11:637–646.
11. Soler R, Rodriguez E, Requejo I, Fernandez R, Raposo L. Magnetic resonance imaging of congenital abnormalities of the thoracic aorta. *Eur Radiol* 1998; 8:540–546.
12. Hansell DM, Lynch DA, McAdams HP, Bankier AA. Imaging of diseases of the chest. 5th ed. Philadelphia: Mosby Elsevier, 2010; 407–420.
13. Sebastia C, Quiroga S, Boye R, Perez-Lafuente M, Castella E, Alvarez-Castells A. Aortic stenosis: spectrum of diseases depicted at multisection CT. *Radiographics* 2003; 23:79–91.
14. Türkvatan A, Akdur PO, Olçer T, Cumhuri T. Coarctation of the aorta in adults: pre-operative evaluation with multidetector CT angiography. *Diagn Interv Radiol* 2009; 15:269–274.
15. Utuk O, Karaca M, Bayturan O, Oncel G, Tezcan UK, Bilge AR. Coarctation of the aorta evaluated with 64-row multidetector computed tomography. *Int J Cardiol* 2006; 111:169–171.
16. Dillman JR, Yarram SG, D'Amico AR, Hernandez RJ. Interrupted aortic arch: spectrum of MRI findings. *AJR Am J Roentgenol* 2008; 190:1467–1474.
17. Moncada R, Shannon M, Miller R, White H, Friedman J, Shuford W. The cervical aortic arch. *AJR Am J Roentgenol* 1975; 125:591–601.
18. Cherian RS, Keshava SN, George O, Joseph E. Cervical aortic arch in a patient with Turner syndrome. *Diagn Interv Radiol* 2010; 16:132–133.
19. Castaner E, Gallardo X, Rimola J, et al. Congenital and acquired pulmonary artery anomalies in the adult: radiologic overview. *Radiographics* 2006; 26:349–371.
20. Davis SD. Proximal interruption of the right pulmonary artery. *Radiology* 2000; 217:437–440.
21. Berdon WE. Rings, slings, and other things: vascular compression of the infant trachea updated from the midcentury to the millennium—the legacy of Robert E. Gross, MD, and Edward B. D. Neuhauser, MD. *Radiology* 2000; 216:624–632.
22. Ahmad Z, Vettukattil J. Pulmonary artery diverticulum: an angiographic marker for Williams syndrome. *Ped Cardiol* 2010; 31:611–614.
23. Pelage JP, Hajjam ME, Lagrange C, et al. Pulmonary artery interventions: an overview. *Radiographics* 2005; 25:1653–1667.
24. Reddy GP, Caputo GR. Diagnosis please. Case 15: congenitally corrected transposition of the great arteries. *Radiology* 1999; 213:102–106.
25. Frank L, Dillman JR, Parish V, et al. Cardiovascular MR imaging of conotruncal anomalies. *Radiographics* 2010; 30:1069–1094.
26. Sridhar PG, Kalyanpur A, Suresh PV, Sharma R, Maheshwari S, Hrudayalaya N. Helical CT evaluation of aortopulmonary window. *Ind J Radiol Imag* 2006 16:4:847–849.